Predictive Simulation of AlGaN/GaN HEMTs

S. Vitanov, V. Palankovski, S. Murad†, T. Rödle†, R. Quay‡, and S. Selberherr*
Advanced Materials and Device Analysis Group at *
*Inst. for Microelectronics, TU Wien, Gußhausstraße 27–29/E360, 1040 Wien, Austria
†ICRF, NXP Semiconductors, Gerstweg 2, 6534 AE Nijmegen, The Netherlands
‡Fraunhofer Inst. for Solid-State Physics (IAF), Tullastraße 72, 79108 Freiburg, Germany

e-mail: vitanov@iue.tuwien.ac.at

***Abstract*— For the development of next-generation AlGaN/GaN based high electron mobility transistors (HEMTs) in industry, reliable software tools for DC and AC simulation are required. Our device simulator Minimos-NT was calibrated against experimental data for this purpose. Subsequently, AC and DC simulations for both scaled devices from the same generation and new generation HEMTs were performed. A good accuracy for all relevant characteristics in comparison to measurement results is achieved.**

I. Introduction

Wide bandgap GaN-based high electron mobility transistors (HEMTs) exhibit power properties which make them eligible for the use in radio frequency applications. The focused extensive investigations in the last years have solved various technology issues and vastly improved the device performance [1], [2]. Nowadays large-scale production of AlGaN/GaN HEMTs is ongoing, however, to further optimize and downscale the structures a reliable simulation tool is needed. Due to the short development cycles a minimal computational effort is advantageous. The two-dimensional device simulator MINIMOS-NT [3] has proven to be a suitable tool for the analysis of heterostructure devices [4], [5]. It was extended for the GaN-material system [6] and a first approach to the DC simulation of HEMTs was made [7]. In this paper we present predictive analyses using a calibrated setup.

II. Device Description

The AlGaN/GaN HEMT technology is based on multi-wafer MOCVD growth on 2-inch semi-insulating SiC substrates based on an Aixtron 2000 multi-wafer reactor. The gate is e-beam defined with a gate length of l_g=150 nm, 300 nm, and 600 nm. Device isolation is achieved by mesa isolation. Fig. 1 gives an example of a typical fully planar HEMT field-plated structure. An $Al_{0.3}Ga_{0.7}N$/GaN heterointerface is grown on top of a thick insulating GaN buffer. All layers are unintentionally doped except the supply layer. The latter is introduced in order to provide additional carriers and to improve the access resistance. We assume a metal diffusion of the metal source and drain contacts reaching the supply layer. The interface charge density is found to be $\approx 1.1\times10^{13}\text{cm}^{-2}$ from the DC transfer characteristics. The positive charge at the channel/spacer interface is compensated by a commensurate negative surface charge at the barrier/cap interface.

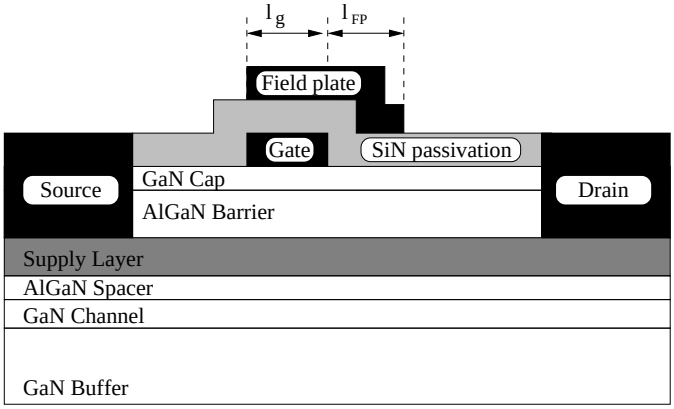

Fig. 1. A schematic layer structure of single heterojunction AlGaN/GaN HEMTs with field-plate investigated in this work.

III. Device Modeling

Since the longitudinal electric field in the channel reaches peak values of above 500 kV/cm, a hydrodynamic approach is required to properly model electron transport and energy relaxation. This approach provides the best accuracy of the results at reasonable computational cost. For example, simulation of a transfer curve, including AC analysis, takes about an hour CPU time on a standard PC with a 2.4 GHz Intel Core 2 Duo processor.

The low-field electron mobility model used in MINIMOS-NT is fitted to own Monte Carlo (MC) simulation results [8]. The high-field mobility model includes energy-dependent electron relaxation times. The hydrodynamic mobility model proposed by Hänsch [9] has been modified to account for GaN specific effects. A more detailed model description is given in [10]. Our model was calibrated to give the best agreement with the velocity-field characteristics and also between simulation and measurement of DC and AC electrical characteristics.

For good control of the sheet carrier concentration in the two-dimensional electron gas (2DEG), the alloy composition and the abruptness of the AlGaN/GaN interface has to be determined. Various methods such as high resolution X-ray diffraction, transmission electron microscopy, and elastic recoil detection have been used [11]–[13]. A good estimate of the effective channel thickness of the conducting region is

1-4244-1022-3/07/$25.00 © 2007 IEEE

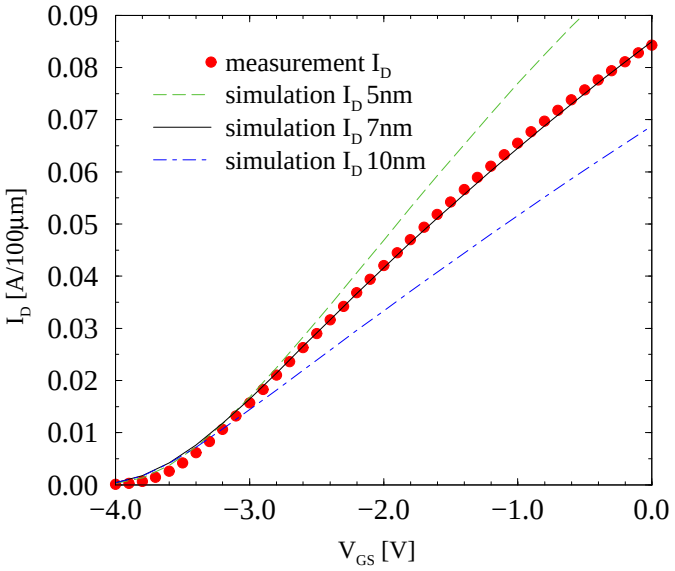

Fig. 2. Measurement data compared to simulation data for different channel thickness.

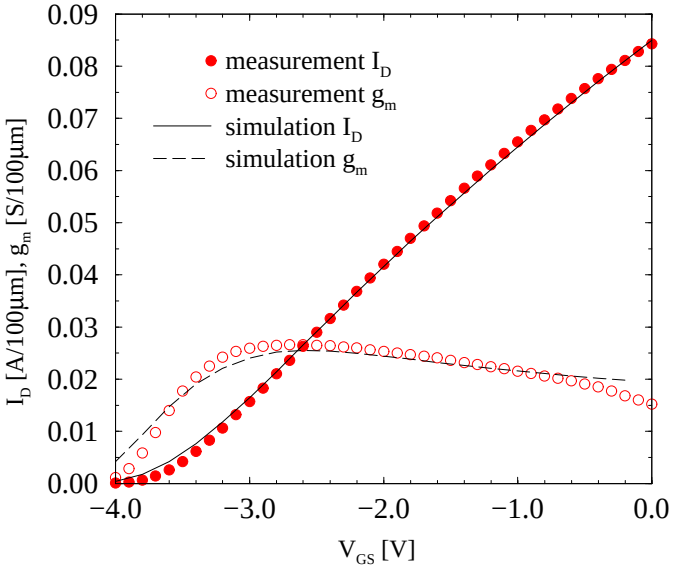

Fig. 3. Calibration of transfer characteristics and transconductance against measured data for Device 1.

required for the simulator. A nominal value for the thickness of the 2DEG region has been given in the literature in the order of 2−3 nm, see for example [14], depending on the Al mole fraction in the AlGaN layer. However, the effective thickness of the conducting region may be wider than the 2DEG, albeit with a lower density. For the purpose of calibrating the simulator to produce the same current density as in the measured devices, a number of 2DEG effective thicknesses were analyzed (see Fig. 2). Thus, a channel thickness of 7 nm was used in all simulations presented in this work.

We further assess the impact of thermionic emission and

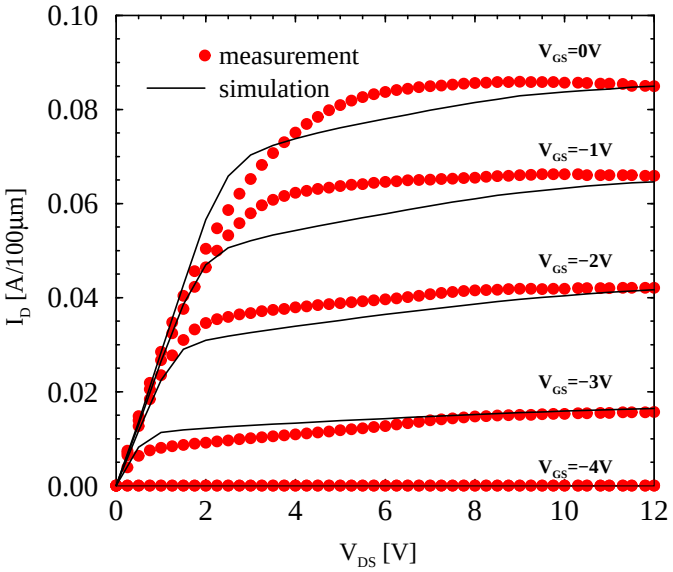

Fig. 4. Calibration of the output characteristics against measured data for Device 1.

field emission (tunneling) effects which critically determine the current transport across the heterojunctions. An optimal tunnel length of 7.5 nm is found. Self-heating effects are accounted for by using a properly adapted ambient temperature.

IV. Simulation Results: Calibration Device

DC and AC measurement data from devices with gate length l_g=0.6 μm, field-plate extension length l_{FP}=0.6 μm, and gate width 100 μm (Device 1) were used for the calibration. The simulation results for the transfer characteristics and transconductance using the calibrated model are compared to the measurement data in Fig. 3 for V_{ds}=12 V. Fig. 4 compares the measured and simulated output characteristics. Quite good an agreement is achieved. The main fitting parameters are the interface charge density and the hydrodynamic mobility model parameter values.

V. Simulation Results: Benchmark Device

Using the calibrated set of models and parameters, several devices with varying geometries were analyzed. Some of these devices were later on produced and characterized. As a particular example, we present predictive results for a downscaled device with l_g=l_{FP}=0.3 μm (Device 2).

Fig. 5 shows the measured and simulated transfer characteristics and transconductance for V_{ds}=12 V. An excellent agreement is achieved for the whole range. Fig. 6 compares the simulated and measured output curves for different gate-source voltages. The simulation tool provided good predictive results.

Fig. 7 compares the measured and simulated cut-off frequency. f_T is overestimated due to an underestimated C_{gs}.

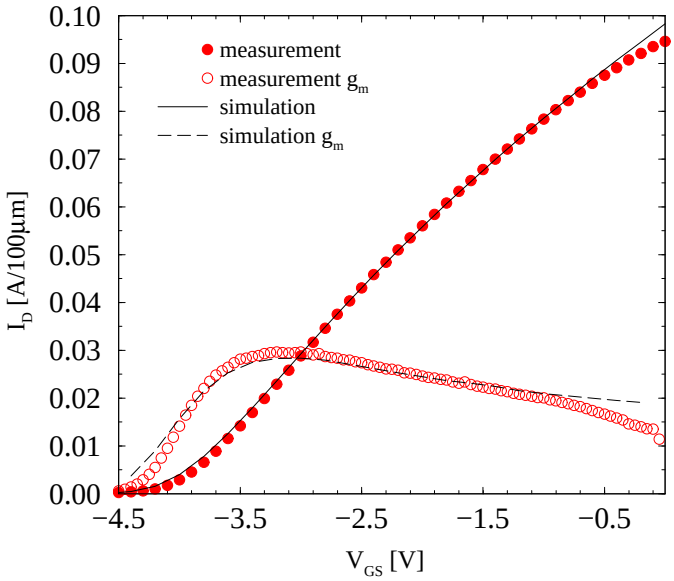

Fig. 5. Predicted transfer characteristics and transconductance compared to measured data for Device 2.

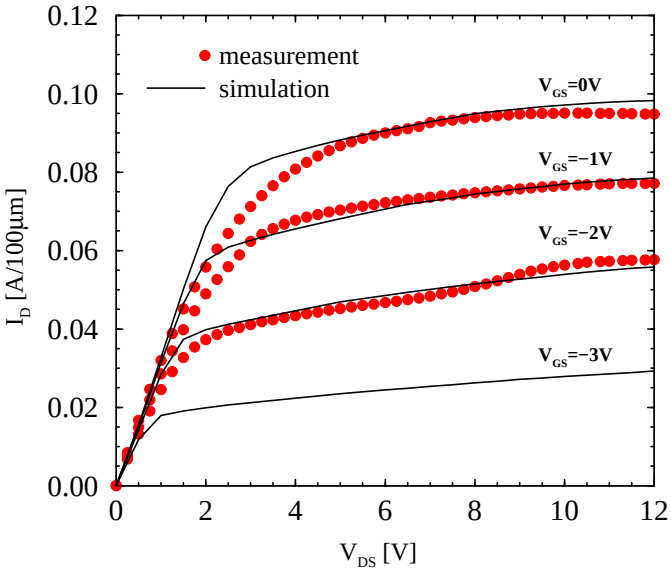

Fig. 6. Predicted output characteristics compared to measured data for Device 2.

VI. Simulation Results: New Generation Device

Using again the calibrated parameter set we studied a l_g=0.5 μm device featuring a source shield-plate (Device 3).

Fig. 8 shows the measured and simulated transfer characteristics for V_{ds}=12 V and V_{ds}=50 V. An excellent agreement is achieved for the whole range in both cases.

Fig. 9 shows the $G_{m,RF}$ measured data compared to the simulated RF transconductance. Again a good agreement is achieved. Additional simulations with slightly reduced AlGaN layer thickness provide better agreement with the experimental data and are a possible explanation for the differences observed.

The input C_{11} and gate-drain capacitance C_{gd} data at Vds=12 V are shown in Fig. 10. While the C_{gd} values exhibit a negligible deviation, C_{gs} is underestimated. Therefrom, the cut-off frequency is overestimated as shown in Fig. 11. Again data for two AlGaN layer setups are provided.

VII. Conclusion

We present a TCAD methodology which allows the design of next-generation GaN HEMTs through predictive simulations with a good accuracy at reasonable computational cost.

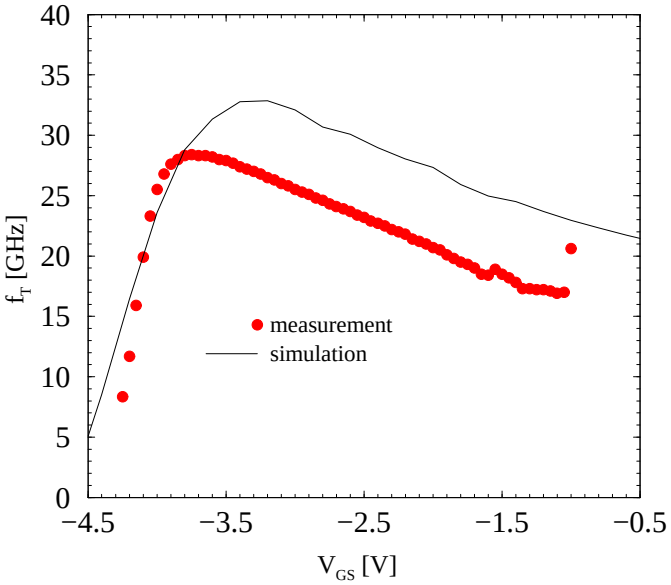

Fig. 7. Predicted cut-off frequency vs. V_{gs} compared to measured data for Device 2.

Acknowledgment

Support by the Austrian Science Funds FWF and BMWK, START Project No.Y247-N13 is acknowledged.

References

[1] Y.F. Wu, B.P. Keller, P. Fini, S. Keller, T.J. Jenkins, L.T. Kehias, S.P. Denbaars, and U.K. Mishra, "High Al-Content AlGaN/GaN MODFET's for Ultrahigh Performance", *IEEE Electron Dev. Lett.*, vol. 19, pp. 50–53, Feb. 1998.

[2] Y.F. Wu, M. Moore, A. Saxler, M. Moore, T. Wisleder, and P. Parikh, "40-W/mm Double Field-Plated GaN HEMTs", in *Proc. 64th IEEE Device Research Conf.*, State College, PA, USA, pp. 151–152, June 2006.

[3] *Institut für Mikroelektronik, Technische Universität Wien. (2002) Minimos-NT Device and Circuit Simulator, User's Guide, Release 2.0.*, http://www.iue.tuwien.ac.at/software/minimos-nt.

[4] V. Palankovski, R. Quay, and S. Selberherr, "Industrial Application of Heterostructure Device Simulation", *IEEE J. Solid-State Circuits*, vol. 36, no. 9, pp. 1365–1370, (invited), Sept. 2001.

[5] V. Palankovski and R. Quay, *Analysis and Simulation of Heterostructure Devices*. Wien, New York: Springer, 2004.

[6] S. Vitanov, V. Palankovski, R. Quay, and E. Langer, "Modeling of Electron Transport in GaN-based Materials and Devices", in *28th Intl.Conf. on the Physics of Semiconductors*, p. 244, July 2006.

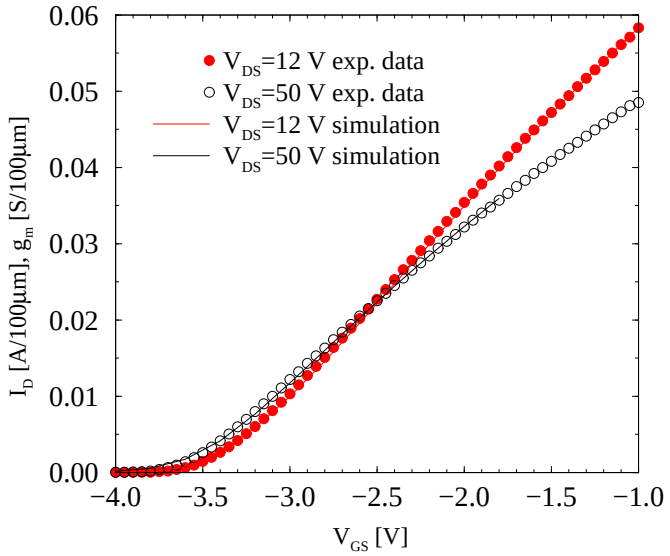

Fig. 8. Predicted transfer characteristics and compared to measured data for Device 3.

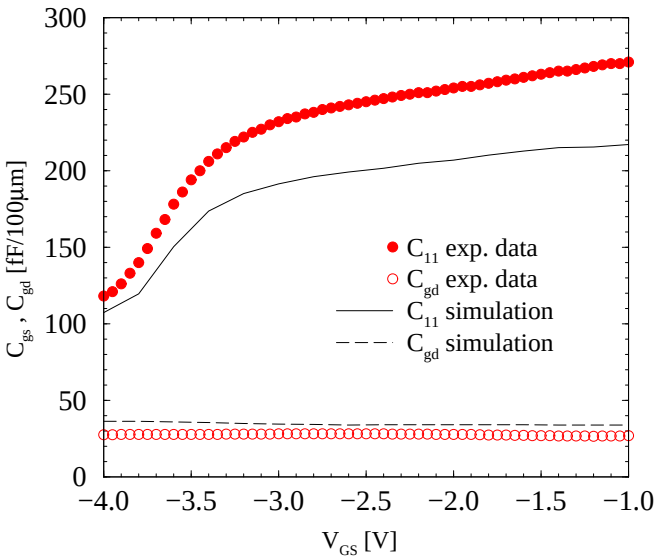

Fig. 10. Predicted capacitances C_{11} and C_{gd} compared to measured data for Device 3.

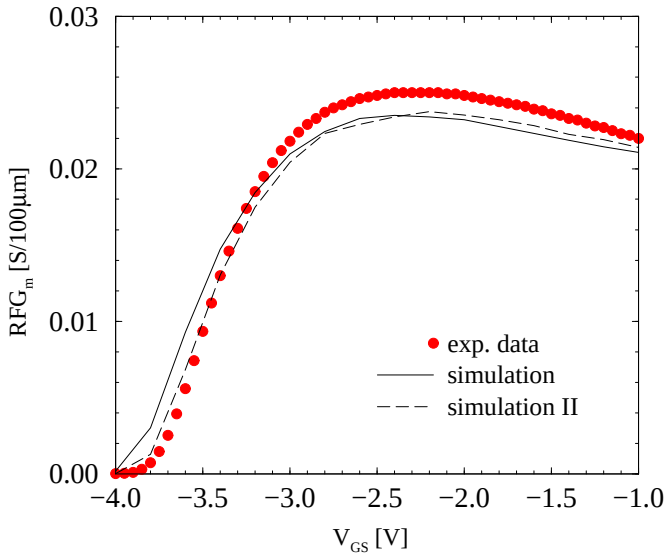

Fig. 9. Predicted RF transconductance compared to measured data for Device 3.

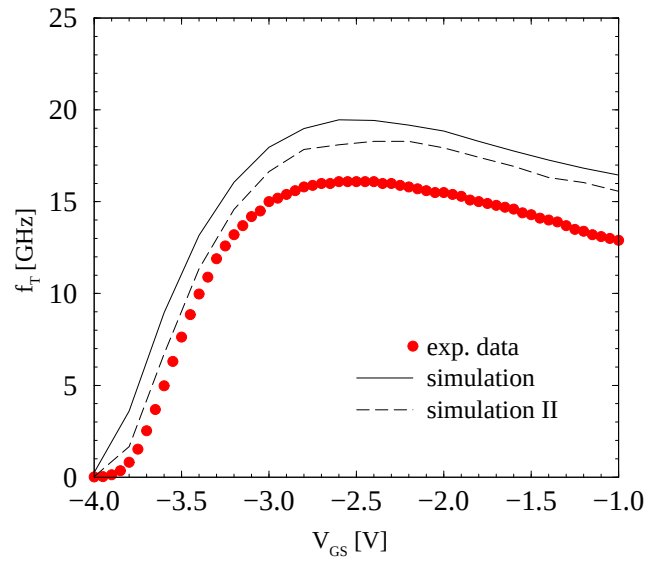

Fig. 11. Predicted cut-off frequency f_T vs. V_{gs} compared to measured data for Device 3.

[7] V. Palankovski, S. Vitanov, and R. Quay, "Field-Plate Optimization of AlGaN/GaN HEMTs", in *Tech.Dig. IEEE Compound Semiconductor IC Symp.*, pp. 107–110, Nov. 2006.

[8] V. Palankovski, A. Marchlewski, E. Ungersböck, and S. Selberherr, "Identification of Transport Parameters for Gallium Nitride Based Semiconductor Devices", in *Proc. 5th MATHMOD*, CDROM, Vienna, pp. 14-1–14-9, Feb. 2006.

[9] W. Hänsch, M. Orlowski, and W. Weber, "The Hot-Electron Problem in Submicron MOSFET", *18th ESSDERC*, pp. 597–606, Sep. 1988.

[10] S. Vitanov, V. Palankovski, S. Murad, T. Rödle, R. Quay, and S. Selberherr, "Hydrodynamic Modeling of AlGaN/GaN HEMTs", in *Proc. Intl.Conf. on Simulation of Semiconductor Processes and Devices*, Wien - New York, Springer, pp. 273–276, Sep. 2007.

[11] O. Ambacher, B. Foutz, J. Smart, J.R. Shealy, N.G. Weimann, K. Chu, M. Murphy, A.J. Sierakowski, W.J. Schaff, L.F. Eastman, R. Dimitrov, A. Mitchell, and M. Stutzmann, "Two-Dimensional Electron Gases Induced by Spontaneous and Piezoelectric Polarization in Undoped and Doped AlGaN/GaN Heterostructures", in *J. Appl. Phys.* , vol. 87, pp. 334–344, Jan. 2000.

[12] D. Jena, I. Smorchkova, A.C. Gossard, and U.K. Mishra, "Electron Transport in III-V Nitride Two-Dimensional Electron Gases", in *Phys. Stat. Sol. B*, vol. 228, pp. 617–619, Jan. 2001.

[13] I. Smorchkova, C.R. Elsass, J.P. Ibbetson, R. Vetury, B. Heying, P. Fini, E. Haus, S.P. DenBaars, J.S. Speck, and U.K. Mishra, "Polarization Induced Charge and Electron Mobility in AlGaN/GaN Heterostructures Grown by Plasma-Assisted Molecular-Beam Epitaxy", in *J. Appl. Phys.*, vol. 86, pp. 4520–4526, Oct. 1999.

[14] B. Jogai, "Influence of Surface States on the Two-Dimensional Electron Gas in AlGaN/GaN Heterojunction Field-Effect Transistors", in *J. Appl. Phys.*, vol. 93, pp. 1631–1635, 2003.